# Liquid crystal phase behavior of a DNA dodecamer and the chromonic dye Sunset Yellow

Joseph G. Theis, Gregory P. Smith, Youngwoo Yi, David M. Walba, and Noel A. Clark

Phys. Rev. E **98**, 042701 — Published 8 October 2018

DOI: 10.1103/PhysRevE.98.042701

# Liquid crystal phase behavior of a DNA dodecamer and the chromonic dye Sunset Yellow

Joseph G. Theis,* Gregory P. Smith, Youngwoo Yi, David M. Walba, and Noel A. Clark†
*Soft Materials Research Center, Department of Physics*
*University of Colorado Boulder, Boulder, Colorado 80309*
(Dated: September 18, 2018)

Sunset Yellow (SSY), is an aromatic heterocycle nano-sheet functionalized by hydrophilic sulphanate groups. SSY forms chromonic stacks and liquid crystal (LC) phases in aqueous solution. The DNA oligomer 5'-GCGCTTAAGCGC-3' is a self-complementary strand which forms duplexed B-form helices in aqueous solution, which, similarly, aggregate into chromonic stacks and form LC phases. Binary aqueous solutions of these two molecules were investigated using polarized optical microscopy, x-ray diffraction, and spectroscopy. At lower solute concentrations and/or higher temperatures these solutions form uniformly mixed single phases, including isotropic, chiral nematic, and hexagonal columnar LCs. At higher solute concentrations and/or lower temperatures, the uniform columnar solution separates into two columnar phases, one containing SSY with trace DNA and the other containing both SSY and DNA aggregates. The study of these solutions indicates that the mixed and unmixed phases are composed of single component SSY or DNA chromonic stacks, with the DNA stacks containing a small fraction of intercalated SSY, evidenced by structurally induced circular dichroism in the SSY absorption band. In the columnar monophase, the hexagonal lattice sites are occupied randomly by either DNA or SSY columns, with the column spacing varying continuously with the SSY-DNA mass ratio. The results demonstrate significant selectivity in the chromonic stacking of both molecules. The binding mode of these chromonic LCs may have applications to adaptive optics and nucleic acid chemistry.

## I. INTRODUCTION

The self-assembly of chromonic dyes and short DNA oligonucleotides into well-ordered liquid crystal (LC) phases has attracted significant attention due to the diversity of mesophases and myriad of applications within optics, materials science, and evolutionary biology [1–3]. These soft materials are lyotropic solutions, meaning that there is a host solvent and that phase boundaries are temperature and concentration dependent. Chromonic molecules are characteristically flat, with aromatic hydrocarbon rings lying in the same plane. These planar molecules stack to form rod-shaped aggregates in water due to $\pi$ stacking about the aromatic cores [4]. In solution, spherocylinders with an anisotropy, quantified by the length over the diameter L/D, greater than 4.7 will spontaneously transition to the nematic LC mesophase ($N$) when the spherocylinders reach a critical density [5, 6]. Chromonic dyes are not sufficiently anisotropic to form these phases as monomers. However, the chromonic stacking of these monomers into long aggregates provides the necessary anisotropy to form LC phases.

Sunset Yellow FCF (SSY) is a commonly studied chromonic, azo dye that is also used as a colorant in food and cosmetics [7–10]. The planar chemical structure of SSY is shown in Fig. 1(a). At 20 °C and 295 mg/mL, SSY transitions from an isotropic fluid ($I$) to $N$, where the aggregates have orientational order [8, 9]. From $N$, SSY transitions to the hexagonal columnar mesophase

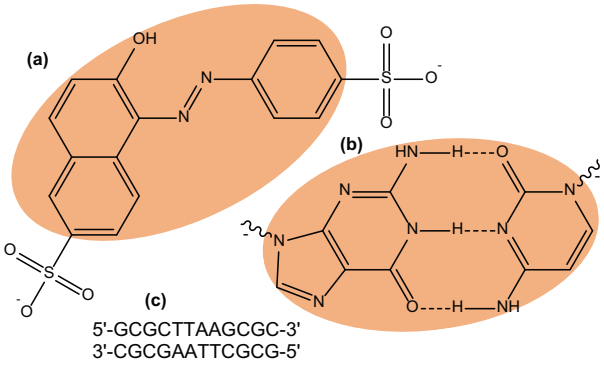


FIG. 1. Chemical structure of (a) SSY and (b) Guanine (left) hydrogen bonded to Cytosine (right). The aromatic heterocycles (orange) lie in the plane of the paper. (c) rDD sequence duplexed to rDD sequence.

($M$) at 450 mg/mL, where the aggregates are positionally ordered on a two-dimensional hexatic lattice [8, 9]. These transitions are driven by the excluded volume's contribution to the entropy of the phase [5]. Reverse Dickerson Dodecamer (rDD) is a single strand of 12 DNA bases. The sequence of rDD (5'-GCG CTT AAG CGC-3') is self-complementary, which facilitates the base-pairing between two single strands of rDD to form the familiar B-form double helix structure [2]. The chemical structure of a G-C base pair is shown in Fig. 1(b). The same forces that cause SSY and other chromonic dyes to aggregate also cause rDD duplexes to aggregate, stacking normal to the plane of the aromatic nucleobases with

* joseph.theis@colorado.edu
† noel.clark@colorado.edu

the negatively charged phosphate groups on the periphery. At 20 °C and 200 mg/mL, rDD transitions from $I$ to cholesteric nematic ($N^*$) where the nematic director rotates between adjacent planes of coaligned aggregates, giving the mesophase a structural chirality with a pitch that can range from nanometers to microns. From $N^*$, rDD transitions to $M$ at 320 mg/mL. Given the dimensions of duplexed DNA, it would require approximately 28 base pairs (bp) to satisfy L/D > 4.7. The existence of LC phases for these short oligonucleotides demonstrates that the duplexes undergo the same chromonic stacking as the dyes.

This work describes the entire LC phase space of mixtures of SSY and rDD. These mixtures were inspired by the similar molecular structure, chromonic stacking, and LC phase behavior of the two materials. Many LC forming molecules are approximated well as hard spherocylinders or, in two dimensions, as hard disks. For identical rods, the $N$ and $M$ phases predictably minimize the free energy. For mixtures of spherocylinders of different lengths and radii (polydisperse mixtures), the arrangement of the species is more complicated. The resultant rDD-SSY phases provide information on the structure of a binary distribution of radii with polydisperse lengths.

Studying the interactions of any molecule with DNA can provide valuable, biologically relevant information. The use of SSY in food and cosmetics is controversial. Studying mixtures of SSY and oligonucleotides may provide a mechanism behind previously reported toxicity in rat studies [11, 12]. Alternatively, many chromophores and fluorophores that non-covalently bind to DNA can be used to image and manipulate biopolymers for scientific and medical applications. Finally, this work helps to address the origin of complex nucleotide polymers. The condensation and ordering of the liquid crystal phases may have provided the autocatalytic link for the polymerization of RNA before the biological mechanisms existed [13]. It has recently been demonstrated that single nucleotides in solution with their complement are capable of forming LC phases [14]. The work described in this article, while not directly probing the origin-of-life hypothesis, is a study of DNA liquid crystals and their selectivity in aggregation. By mixing molecules of similar structure and size with DNA LCs, we can explore the propensity of DNA to aggregate into homogeneous duplexed rods when competition exists with other organic compounds.

## II. MATERIALS AND METHOD

### A. Materials and Preparation

Sunset Yellow FCF was purchased from Sigma Aldrich. No additional purification was performed. The LC phase diagram for SSY is shown on the back plane of Fig. 6(a). These transitions generally agree with those previously reported [8, 9]. The overall concentrations ($c$) are reported in milligram of total solute per milliliter of sample (solute + solvent) as mg/mL. Our convention, which considers the volume of the molecules is given in Equation 1. The polarized optical microscopy (POM) textures for SSY are shown in Fig. 2(a). SSY is dichroic in the visible spectrum with a pH dependent maximum absorbance at 480 nm and significant shoulder peaks at 520 nm and 430 nm. The dichroism was used to determine the orientation of the optic axis in different domains and also to confirm the presence of SSY in the mixture. SSY is an achiral molecule.

$$c = \frac{m_{ssy} + m_{dna}}{\frac{m_{ssy}}{\rho_{ssy}} + \frac{m_{dna}}{\rho_{dna}} + \frac{m_{water}}{\rho_{water}}}. \quad (1)$$

We synthesized the single-stranded rDD at the Soft Materials Research Center (SMRC), using the Caruthers Method [15]. The optical density of the purified and lyophilized rDD was 26.39 OD/mg. MALDI-TOF mass spectroscopy confirmed the rDD mass to within the error of the instrument. The phase diagram for rDD can be found on the front plane of Fig. 6(a). The POM textures are shown in Fig. 2(b).

rDD and SSY were mixed in powder form and then DI water was added to obtain the desired concentration. The convention in this work is to label the ratio of the species as the fraction of solute mass that is SSY ($\mathrm{mf}_{ssy}$). For some viscous, high concentration mixtures the samples were prepared at lower concentrations, transferred to a cell or capillary, and then allowed to evaporate to reach the desired concentration.

### B. Experimental Methods

The primary means of observing the samples was POM and x-ray diffraction (XRD). For POM, samples were observed in cells or capillaries between crossed polarizer and analyzer. The analyzer was removed for dichroism measurements. For cells, a thin cover slip was placed over the sample on 5 $\mu$m spacers. Mineral oil was placed around the cover slip to slow evaporation. With a temperature-controlled stage, this technique filled in much of the phase diagram.

XRD measurements were performed at the Advanced Light Source at Lawrence Berkeley National Laboratory on samples in sealed capillaries. The samples were unaligned resulting in a powder scattering pattern. Thus, the 2D data from the areal detector was compressed to 1D via circularly averaging about the beam center. The lattice parameters were determined from Lorentzian functions fitted to the raw 1D data. The coherence length $\xi_\ell$, defined as the distance at which the standard deviation from the lattice equals the associated lattice spacing, was calculated as the inverse of the full width at half maximum.

In addition to these primary measurement techniques, multiple spectroscopic assays were performed including

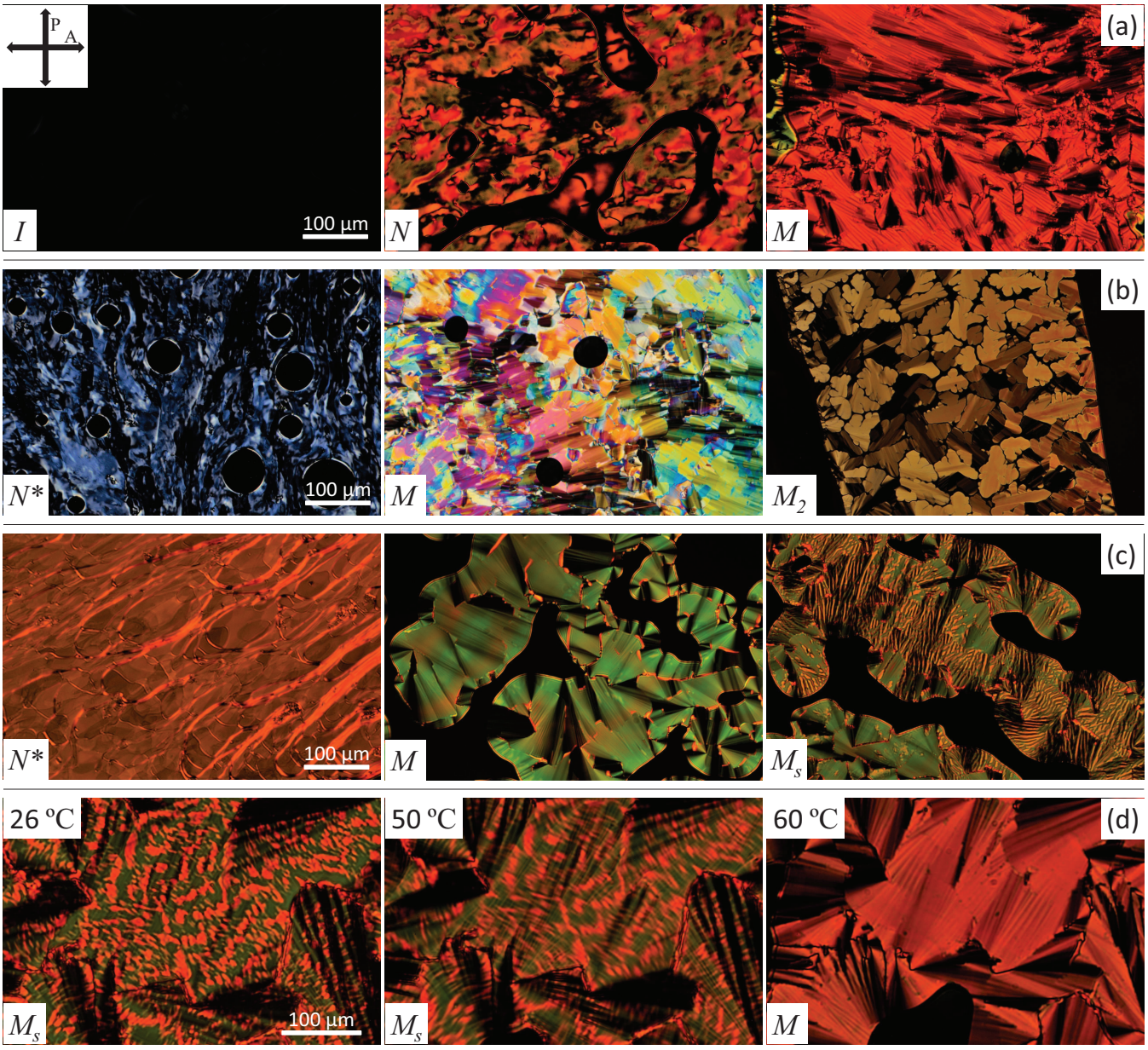


FIG. 2. (a, b, c) POM textures with concentration increasing from left to right at room temperature. (a) Pure SSY ($mf_{ssy}$ = 1) in *I*, *N*, and *M*. (b) Pure rDD $mf_{ssy}$ = 0 in *N**, *M*, and $M_2$. (c) Mixture at $mf_{ssy}$ = 0.57 in *N**, *M*, and $M_s$. (d) POM textures at selected temperatures during heating of $mf_{ssy}$ = 0.57 with a transition from $M_s$ to *M*.

circular dichroism spectroscopy (CD), absorption spectroscopy, and scanning Raman microscopy. Absorbance and CD spectra were measured by a Chirascan CD Spectrometer in 0.5 mm quartz cuvettes.

## III. RESULTS AND DISCUSSION

### A. Phase Behavior Overview

The phase behavior of the rDD-SSY mixture was explored as a function of 3 variables: temperature, overall concentration, and ratio of the two species. The concentrations ranged from 0.5 mg/mL to 800mg/mL. The temperatures covered 20 °C to 100 °C. The ratios spanned pure SSY ($mf_{ssy}$ = 1) to pure rDD ($mf_{ssy}$ = 0). In all mesophases, the SSY molecules form homogeneous

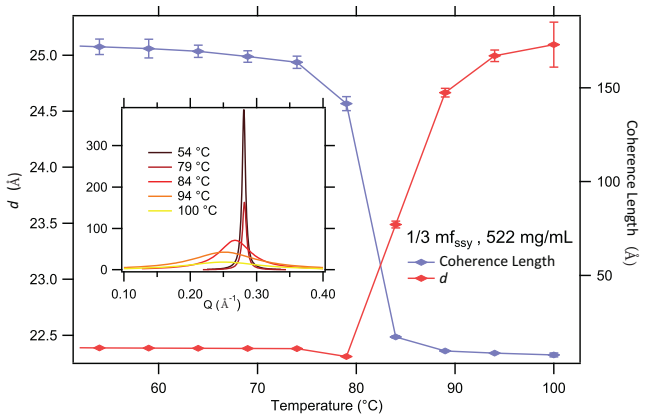


FIG. 3. $d$ (left axis) and coherence length (right axis) as a function of temperature for $\mathrm{mf}_{ssy} = 1/3$ and $c = 522$ mg/mL during cooling. The inset plot shows the corresponding fitted Lorentzian peaks in Q space.

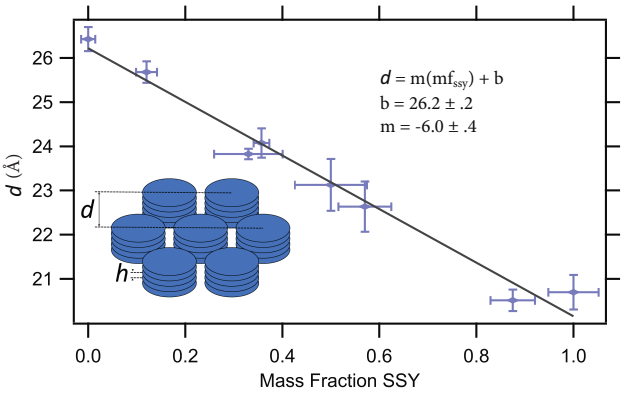


FIG. 4. $d$ as a function $\mathrm{mf}_{ssy}$ in $M$. The values of $d$ were extrapolated to $c = 462$ mg/mL using the relationship in Equation 2. This linear relationship indicates that the two molecules segregate into homogeneous columns that are mixed randomly at the hexagonal lattice sites. The inset figure shows a simplified $M$ lattice with $d$ and $h$ labelled.

chromonic stacks. The rDD duplexes forms nearly homogeneous stacks with trace SSY. These rod-shaped aggregates exhibit $I$, $N$, $N^*$, $M$, $M_2$, and a biphasic, coaligned columnar, $M_s$. The structures and POM textures of the monophase mixtures are presented first, followed by a description of $M_s$, and concluding with a discussion of the binding mode of the two molecules.

### B. Monophase Mixtures

POM textures for pure SSY, pure rDD, and a mixture with $\mathrm{mf}_{ssy} = 0.57$ are shown in Fig. 2(a), (b), and (c), respectively. Across all ratios, the $N^*$ and $M$ phases showed uniform dichroism and birefringence, indicating that the composition is uniform on an optical scale. The nematic phase was chiral due to the presence of the chiral rDD duplex. In addition to $N^*$ and $M$ phases, pure rDD transitions to a second columnar phase, denoted $M_2$, shown in Fig. 2(b), characterized by stronger positional correlation between the columns [14].

The inset plot in Fig. 3 shows the small angle x-ray scattering of a mixture ($\mathrm{mf}_{ssy} = 1/3$, $c = 522$ mg/mL) at selected temperatures during cooling. The Q vector of these peaks is related to the spacing between layers of columns ($d$) in $M$ via $d = 2\pi/Q$. This is the h=0, k=1 plane in the hexagonal lattice. Below 82 °C, the narrow single peak with $d$ comparable to the molecular diameter indicates the aggregates are in a monophasic $M$. Above 82 °C, the broad peak at lower Q is characteristic of $N^*$. At 82 ±2°C, the sample transitions from $N^*$ to $M$. This mesophase change is also apparent in the plots of $d$ and $\xi_\ell$, which reflect the tightening of the spacing and an increased order of the phase, respectively. In both the $N^*$ and $M$ phases, the single peak indicates that the two aggregates are in a well-mixed monophase. $d$ in $M$ as a function of $\mathrm{mf}_{ssy}$ is shown in Fig. 4. The concentrations of the samples in this plot were normalized to 462 mg/mL. This normalization depends on the fact that the spacing between molecules within an aggregate ($h$) does not vary with concentration for either molecule. The incompressibility along $h$ means that, in the columnar phase, the concentration will be inversely proportional to the area per aggregate given in Equation 2. The stacking height for both molecules is $3.3 \pm 0.1$ Å. $d$ is linear with respect to the $\mathrm{mf}_{ssy}$, indicating that the two molecules primarily segregate into homogeneous stacks that are randomly mixed at the 2D hexagonal lattice sites. The inset figure in Fig. 4 shows $d$ and $h$ for a discotic $M$.

$$1/c \propto area/column = 2d^2/\sqrt{3}. \qquad (2)$$

In previous work, our group found that mixtures of SSY and disodium cromoglycate (DSCG), another ubiquitous lyotropic, chromonic LC, phase separate upon transition from $I$ to $N$ [16]. These molecules are structurally more similar than SSY and rDD, so the discovery of uniform $I$, $N^*$, and $M$ phases for mixtures of rDD and SSY was intriguing.

### C. Biphase Mixtures

At higher concentrations and/or lower temperatures, the mixed columnar phase separates into an equilibrium biphasic columnar ($M_s$). This phase separation is visible in the POM textures. Thin lines appear and then grow parallel to the columnar director, eventually forming irregularly shaped domains with a significantly different birefringence and absorbance. The texture of $M_s$ is shown in Fig. 2(c) and (d) for a sample with $\mathrm{mf}_{ssy} = 0.57$. This biphasic mesophase persists until the LC solidifies. The separation is thermally reversible. The mixing temperature $\mathrm{T}_c$, at which $M_s \longrightarrow M$, is a function of $c$ and

$mf_{ssy}$. Remixing upon heating is shown in Fig. 2(d) for a sample with $mf_{ssy} = 0.57$ where $T_c = 60$ °C. Upon cooling, the samples return to $M_s$. The same angular dependence of the SSY dichroism reveals that the columns maintain a common director across domain boundaries and that SSY is present in both domains.

Raman microscopy and absorption spectroscopy with spatial resolutions smaller than the separated domain size were used to probe the composition in cells prepared at $mf_{ssy} = 0.57$. The Raman spectra was saturated by the SSY signature in both domains, while the absorption spectra showed a 45% increase in absorption at 480 nm for the SSY rich domains. The convention will be to describe the domains in the biphase with less SSY as rDD rich for clarity.

XRD measurements of a high concentration mixture showed evidence of the biphase. Figure 5 shows the small angle x-ray scattering of a sample with $c = 562$ mg/mL and $mf_{ssy} = 0.66$ during heating. The two peaks that exist at 40 °C at Q = 0.296 Å$^{-1}$ and 0.332 Å$^{-1}$ correspond to the rDD rich and SSY rich regions, respectively. The spacing and coherence length of these domains indicates that both are hexagonal columnar. The spacing of the SSY rich region requires nearly pure SSY packing (see Fig. 4). As this sample was heated, $h$ remained constant while the difference in $d$ between the domains decreased. The rDD rich domain had a larger shift in $d$, indicating that the SSY aggregates diffuse into the rDD rich domains, decreasing $d$ due to the tighter packing of the SSY aggregates. It is possible that some duplexes melted to single strands, which would also contribute to this tightening. A single peak at 86 °C indicates that the molecules were completely remixed and the sample was monophasic. This second order binary phase transition represents a competition between the entropy of mixing (maximized by $M$) and the entropy associated with the excluded volume (maximized by $M_s$), which favors columns of the same diameter. The phase diagram for this mixture as a function of c, $mf_{ssy}$, and temperature is shown in Fig. 6.

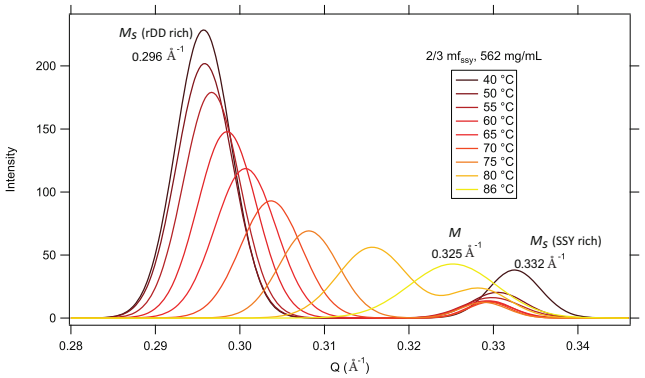


FIG. 5. Fitted Lorentzians for the XRD peaks in the columnar range for $mf_{ssy} = 2/3$ and $c = 562$ mg/mL during heating. There are two peaks corresponding to the different spacing in the SSY rich and the rDD domains until 86 °C where the domains mix and return to a single column spacing in $M$.

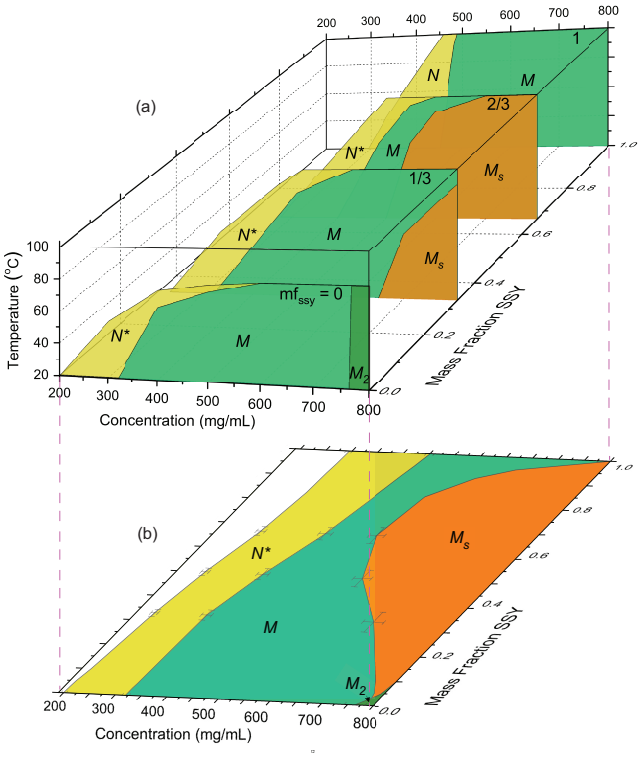


FIG. 6. (a) Phases of rDD-SSY mixture as a function of concentration, $mf_{ssy}$, and temperature at four selected mass fractions. The plane at 20 °C is extruded beneath in (b) where the phases of rDD-SSY are shown as a function of concentration and $mf_{ssy}$.

### D. Binding Mode

The presence of SSY in the rDD rich domains of $M_s$, evidenced by the spacing $d$, the visible dichroism, and the absorption, prompted us to explore the disposition of the SSY. It has been reported that SSY can non-covalently bind to long calf-thymus DNA strands for mixtures with $c \sim 10$ $\mu$g/mL [17, 18]. To explore the propensity of SSY to bind to our dodecamer and to deduce the binding mode, we measured the CD and absorbance spectra of the mixture in water. SSY is achiral as a monomer and in aggregates and, therefore, has no CD spectra [7]. Duplexed rDD has a negative band at 252 nm, corresponding to the B-form, right-handed helix and a positive band at 276 nm, corresponding to the $\pi$ electron base stacking [19, 20]. The magnitude of these peaks increased linearly with [rDD] until the detector saturated at [rDD] = 5 mg/mL. rDD does not absorb in the visible spectrum. SSY absorbs in the visible and UV spectrum. Therefore, we could see if the SSY molecules interacted with the chiral rDD environment by observing the visible band. The CD and absorbance spectra of SSY ([SSY] = 0.5 mg/mL)

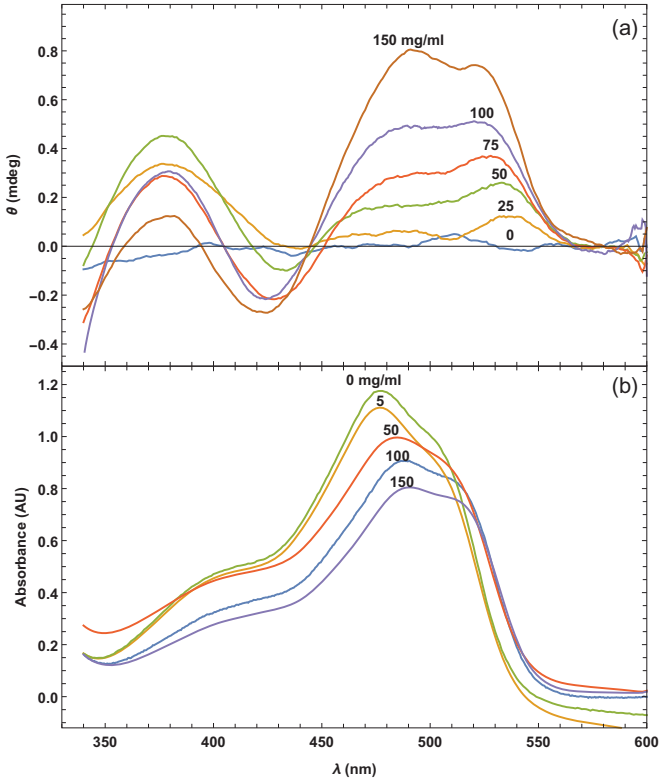


FIG. 7. Smoothed (a) CD and (b) absorbance spectra of rDD-SSY mixtures. [SSY] = 0.5 mg/mL. [rDD] in mg/mL are labeled on the respective curves. CD spectra has saturated by [rDD] = 150 mg/mL. Only SSY absorbs in this domain, indicating that the achiral SSY molecules are binding to the chiral rDD duplexes. These solutions are *I*.

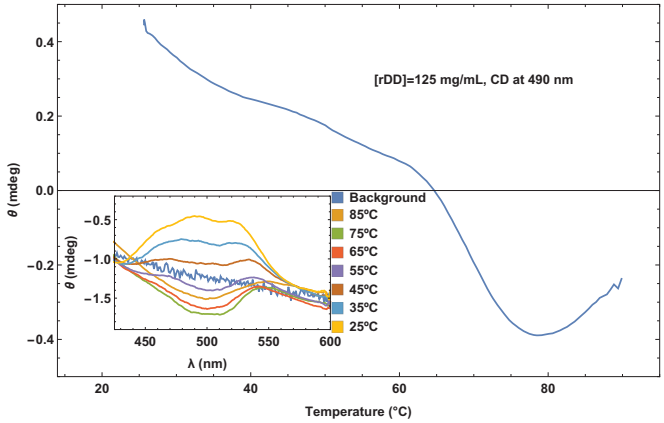


FIG. 8. Ellipticity at 490 nm during heating at 2 °C/min for [SSY] = 0.5 mg/ml and [rDD] = 150 mg/ml. The inset graph shows smoothed CD spectra and the background signal during cooling. The handedness switches from right to left during cooling. Above 79 °C, the induced CD weakens due to dissociation of the SSY from the rDD.

during titration with rDD are shown in Fig. 7(a) and (b), respectively. The induced CD of SSY, evidenced by the positive bands developing at 490 nm and 520 nm, demonstrates that SSY does form complexes with rDD molecules. The binding saturates when [rDD] = 140 ± 10 mg/mL or $\mathrm{mf}_{ssy} = 0.004 \pm 0.001$. This indicates that the maximum binding density of SSY is 1 monomer for every 19 duplexes. The hypochromic and bathochromic shift of the peak absorption at 490 nm in Fig. 7(b) also saturates at [rDD] = 140 mg/mL. This shift in absorption is characteristic of intercalation [20, 21] and is different than the absorption shifts that occur upon aggregation [10]. SSY fluorescence has been observed to increase by a factor of 5 upon titration with calf-thymus DNA [18]. Finally, the visible dichroism of the DNA rich regions in $M_2$ indicates that the optic axis of the SSY molecules lie in the same plane as the nucleotides. Taken together, we hypothesize that SSY is intercalating between bases within the rDD duplex and/or between aggregated duplexes. The relatively low binding density may be due to defect dependent binding sites on the DNA helix. The duplex bound SSY molecules are present in all LC phases and may contribute to the miscibility of the molecules.

Upon heating the induced chirality of the SSY changes handedness, going from left to right handed. The maximum negative ellipticity occurs at 78 °C. Above this temperature the signal begins to weaken possibly due to the dissociation of the SSY from the helix. This phenomenon may be due to the melting of the double stranded DNA or a change in the binding mode. The original handedness returns upon cooling. This process is shown in Fig. 8. We cannot rule out the possibility of groove binding or multiple binding modes. The tunable induced chirality of this mixture is an exciting discovery that will be the subject of future research.

## IV. CONCLUSION

Mixtures of SSY and rDD DNA exhibit well-mixed *I*, *N**, and *M* phases. These homogeneous phases consist of aggregates of pure SSY and aggregates of duplexed rDD with trace SSY intercalated into the columns. As the inter-column spacing decreases at higher concentrations and/or lower temperatures, excess SSY separates from the mixture and forms regions of nearly pure SSY *M*. The rDD rich regions still contain SSY as an intercalant and in homogeneous stacks. The boundaries between the phases form parallel to their shared columnar director. The texture of all phases depends on the overall concentration, the ratio of the two species, and the history of the sample. The miscibility and the intercalative capacity of the SSY demonstrate the high degree of similarity between the molecular structures and chromonic LC ordering of these two molecules. SSY may be an effective and cheap model for the behavior of short or even mono-nucleotides in solution. The dodecamer does, however, exhibit the B-form helix in the presence of a competitive chromonic, organic molecule. In the context of the prebiotic origin of nucleic acid polymers, this result demonstrates the

potential for auto-catalyzed ligation of short nucleic acid oligomers in an impure, prebiotic "soup"[13]. Finally, the induced structural chirality in the SSY-rDD mixture and the temperature dependent ICD response have exciting potential in adaptive optics and nucleic acid chemistry.

## ACKNOWLEDGMENTS

This work supported by NSF Biomaterials Grant DMR-1611272 and by the Soft Materials Research Center under NSF MRSEC Grant DMR-1420736. This research used beamline 7.3.3 of the Advanced Light Source, which is a DOE Office of Science User Facility under contract no. DE-AC02-05CH11231.

[1] H.-S. Park and O. D. Lavrentovich, *Lyotropic chromonic liquid crystals: Emerging applications* (Wiley Online Library, 2012) pp. 449–484.
[2] M. Nakata, G. Zanchetta, B. D. Chapman, C. D. Jones, J. O. Cross, R. Pindak, T. Bellini, and N. A. Clark, Science **318**, 1276 (2007).
[3] S. Shiyanovskii, O. Lavrentovich, T. Schneider, T. Ishikawa, I. Smalyukh, C. Woolverton, G. Niehaus, and K. Doane, Mol. Cryst. Liq. Cryst. **434**, 259 (2005).
[4] J. Lydon, J. Mater. Chem. **20**, 10071 (2010).
[5] L. Onsager, Ann. N.Y. Acad. Sci. **51**, 627 (1949).
[6] P. Bolhuis and D. Frenkel, J. Chem. Phys. **106**, 666 (1997).
[7] F. Chami and M. R. Wilson, J. Am. Chem. Soc. **132**, 7794 (2010).
[8] D. Edwards, J. Jones, O. Lozman, A. Ormerod, M. Sintyureva, and G. Tiddy, J. Phys. Chem. B **112**, 14628 (2008).
[9] H.-S. Park, S.-W. Kang, L. Tortora, Y. Nastishin, D. Finotello, S. Kumar, and O. D. Lavrentovich, J. Phys. Chem. B **112**, 16307 (2008).
[10] V. R. Horowitz, L. A. Janowitz, A. L. Modic, P. A. Heiney, and P. J. Collings, Phys. Rev. E **72**, 041710 (2005).
[11] E. G. Helal, Egypt J. Hosp. Med. **2**, 23 (2001).
[12] N. Mathur, V. Chaudhary, M. Mehta, and S. Gupta, Biochemical Cellular Archive **5**, 197 (2005).
[13] T. P. Fraccia, G. P. Smith, G. Zanchetta, E. Paraboschi, Y. Yi, D. M. Walba, G. Dieci, N. A. Clark, and T. Bellini, Nature communications **6**, 6424 (2015).
[14] G. P. Smith and N. A. Clark, (unpublished).
[15] M. H. Caruthers, J. Biol. Chem. **288**, 1420 (2013).
[16] A. Yamaguchi, G. P. Smith, Y. Yi, C. Xu, S. Biffi, F. Serra, T. Bellini, C. Zhu, and N. A. Clark, Phys. Rev. E **93**, 012704 (2016).
[17] S. Kashanian, S. H. Zeidali, K. Omidfar, and N. Shahabadi, Mol. Biol. Rep. **39**, 10045 (2012).
[18] S. Asaadi and R. Hajian, J. Mol. Struct. **1146**, 861 (2017).
[19] S. S. Jain, M. Polak, and N. V. Hud, Nucleic Acids Res. **31**, 4608 (2003).
[20] D. Sarkar, P. Das, S. Basak, and N. Chattopadhyay, J. Phys. Chem. B **112**, 9243 (2008).
[21] S. Parodi, F. Kendall, and C. Nicolini, Nucleic Acids Res. **2**, 477 (1975).